Study of Some Optimal *XFEM* Type Methods

Elie Chahine[1], Patrick Laborde[2], Julien Pommier[1], Yves Renard[1] and Michel Salaün[3]

[1] *INSA, Laboratoire MIP, CNRS UMR 5640, Complexe scientifique de Rangueil, 31077 Toulouse, France; E-mail: {elie.chahine, pommier, renard}@insa-toulouse.fr*
[2] *Université P. Sabatier, Laboratoire MIP, CNRS UMR 5640, 118 route de Narbonne, 31062 Toulouse Cedex 4, France; E-mail: laborde@math.ups-tlse.fr*
[3] *ENSICA, 1 pl. Émile Blouin, 31056 Toulouse Cedex 5, France; E-mail: msalaun@ensica.fr*

Abstract. The *XFEM* method in fracture mechanics is revisited. A first improvement is considered using an enlarged fixed enrichment subdomain around the crack tip and a bonding condition for the corresponding degrees of freedom. An efficient numerical integration rule is introduced for the nonsmooth enrichment functions. The lack of accuracy due to the transition layer between the enrichment aera and the rest of the domain leads to consider a pointwise matching condition at the boundary of the subdomain. An optimal numerical rate of convergence is then obtained using such a nonconformal method.

Key words: Fracture, finite elements, XFEM method, optimal rate of convergence, pointwise matching.

1 Introduction

In computational fracture mechanics, the *eXtended Finite Element Method* was introduced in order to use a finite element mesh independent of the crack geometry [2, 8, 15, 16, 19]. A better accuracy was obtained for a lower computational cost thanks to *XFEM* instead of considering a classical finite element method. However, numerical experiments show that the rate of convergence is not improved, when the mesh parameter h goes to zero, for the elasticity problem on a cracked body [18]. So, we are interested in the abilities of the methodology *XFEM* to achieve an *optimal* accuracy for such non-smooth problems. Optimality refers here to an error of the same order than the one given by a classical finite element method for a *smooth* problem.

The principle of the extended finite element method consists in incorporating some *enrichment functions* into the finite element basis. Singular enrichement functions are used to take into account the nonsmooth behavior of the displacement field near the crack tip. In the standard *XFEM*, the size of the enrichment area at the crack

tip vanishes when h goes to zero (the enrichment area is the union of the supports of these new singular basis functions). So the influence in the global error of the enrichment decreases with h, which explains the above-mentioned unsatisfactory numerical behavior. To overcome the difficulty, a first variant of *XFEM* was considered in which a whole fixed area (independent of h) around the crack tip is enriched [3, 11].

In the present paper, some improvements of the previous approach are studied in order to obtain better computational performances (in terms of numerical rate of convergence, number of degrees of freedom or well-conditioned system).

The *outline* of the paper is the following. In Section 2, the model problem of a cracked body in linear plane elasticity is considered. Section 3 is devoted to a new *XFEM* type method where the crack tip enrichment functions are localized by using a smooth *cut-off* function. A mathematical result of *optimal* error estimate is stated and confirmed by numerical tests for linear finite elements. In Section 4, a piecewise linear cut-off function is considered for the singular enrichment. The method comes to introduce some *bonding condition* between the enrichment degrees of freedom in *XFEM* with a fixed enrichment area. The numerical rate of convergence is improved for high order finite elements (of degree two or three) with respect to the classical *XFEM* method. However, optimality is not achieved because of the lack of accuracy coming from the elements in the *transition layer* (the finite elements between the enrichment area and the rest of the body). An efficient numerical integration rule for the nonsmooth enrichment functions is presented in Section 5. In the last section, we study a nonconformal method where a *pointwise matching condition* at the boundary of the enriched area takes the place of the transition layer. On a computational test, we then obtain the expected optimality.

2 The Elasticity Problem on a Cracked Domain

Consider the model problem of the equilibrium of a cracked body in plane elasticity. Let Ω be the bounded cracked domain in $\boldsymbol{R}^2$; the crack Γ_C is assumed to be straight. The boundary $\partial\Omega$ of the body is partitioned into Γ_C, Γ_D and Γ_N; a traction free condition is considered on Γ_C, on Γ_D the displacement is prescribed and the surface forces are known on Γ_N (Figure 1).

The weak formulation of the elasticity problem on the cracked domain Ω consists in finding a displacement field $u = (u_1, u_2)$ such that

$$u \in V, \quad a(u, v) = L(v) \quad \forall v \in V, \tag{1}$$

in the space of admissible displacements:

$$V = \{v \ : \ v \in \boldsymbol{H}^1(\Omega), \ v = 0 \ \text{ on } \Gamma_D\}.$$

We have denoted

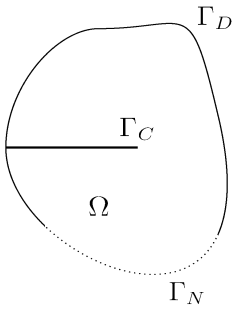

Fig. 1. The cracked domain Ω.

$$a(u, v) = \int_\Omega \sigma(u) : \varepsilon(u)\, d\Omega,$$
$$\sigma(u) = \lambda\, tr\varepsilon(u)\, I + 2\mu\, \varepsilon(u),$$
$$L(v) = \int_\Omega g.v\, d\Omega + \int_{\Gamma_N} f.v\, d\Gamma.$$

The notation $\varepsilon(u)$ stands for the linearized strain tensor, the Lamé coefficients satisfy $\lambda > 0$, $\mu > 0$, the force densities f and g are given on Γ_N and Ω respectively. The inner product of vectors in $\boldsymbol{R}^2$ is written $u.v = \sum_i u_i\, v_i$ and the associated norm $|.|$; for tensors, the inner product is denoted as usually $\sigma : \varepsilon = \sum_{ij} \sigma_{ij}\, \varepsilon_{ij}$. Finally, the functional spaces for vector-valued functions are distinguished by bold characters, e.g. $\boldsymbol{H}^s(\Omega) = H^s(\Omega; \boldsymbol{R}^2)$ equipped with its canonical norm $\|.\|_{s,\Omega}$.

There exists a unique displacement solution u to (1) under standard assumptions, i.e. mes $\Gamma_D > 0$, f and g defining a continuous linear form $L(.)$ on V. Assuming smoothness conditions on the data, the solution u can be written as a sum of a singular part u^* and regular one $u - u^*$ satisfying the following properties:

$$u^* = K_I\, u_I + K_{II}\, u_{II}, \tag{2}$$

$$u - u^* \in \boldsymbol{H}^{2+m}(\Omega), \tag{3}$$

for some integer $m \geq 0$ such that (in particular) $g \in \boldsymbol{H}^m(\Omega)$. In the definition of u^*, the constants K_I, K_{II} are the so-called *stress intensity factors* and the displacements u_I, u_{II} denote the *opening modes* of the crack. For a bi-dimensional crack [12, 13]:

$$u_I = \frac{1}{E}\sqrt{\frac{r}{2\pi}}(1+\nu)\begin{pmatrix}\cos\frac{\theta}{2}(3-4\nu-\cos\theta)\\ \sin\frac{\theta}{2}(3-4\nu-\cos\theta)\end{pmatrix}, \tag{4}$$

$$u_{II} = \frac{1}{E}\sqrt{\frac{r}{2\pi}}(1+\nu)\begin{pmatrix}\sin\frac{\theta}{2}(\gamma+2+\cos\theta)\\ \sin\frac{\theta}{2}(\gamma-2+\cos\theta)\end{pmatrix}, \tag{5}$$

in polar coordinates (r, θ) relatively to the crack tip, where ν is the Poisson ratio and the constant γ is equal to $\gamma = 3 - 4\nu$ for the plane stress problem. The normal (respectively tangential) component of function u_I (resp. u_{II}) is discontinuous along the crack. Note that the functions u_I and u_{II} belong to $\boldsymbol{H}^{3/2-\epsilon}(\Omega)$ for any $\epsilon > 0$ (see [9, 10]).

3 The Cut-Off Method

Assume that the *uncracked* body $\overline{\Omega}$ is a polyhedric domain and consider a *regular* triangulation $\mathcal{T}_h$ of $\overline{\Omega}$. The mesh parameter h corresponds to the maximum of the diameters of the triangles in $\mathcal{T}_h$. Denote $\varphi_1 \dots \varphi_N$ the P_k finite element basis functions on the triangulation, where P_k represents the polynomials of degree $k \geq 1$.

Let H be the function defined on Ω, equal to $+1$ on the one side of the crack Γ_C and equal to -1 on the other one:

$$H(x) = \begin{cases} +1 & \text{if } (x - x^*).n > 0, \\ -1 & \text{elsewhere.} \end{cases}$$

In this definition, n is a given normal vector to the crack line. The asymptotic displacement (2) at the crack tip x^* can be written as a linear relation between the following singular functions $F_1, \dots, F_4$ (see (4) and (5)):

$$F_1 = \sqrt{r}\sin\frac{\theta}{2},\ F_2 = \sqrt{r}\cos\frac{\theta}{2},\ F_3 = \sqrt{r}\sin\frac{\theta}{2}\cos\theta,\ F_4 = \sqrt{r}\cos\frac{\theta}{2}\cos\theta.$$

Let us introduce a C^2-function χ satisfying

$$\begin{cases} \chi(r) = 1 & \text{if } r \leq R_0, \\ 0 < \chi_0(r) < 1 & \text{if } R_0 < r < R_1, \\ \chi_0(r) = 0 & \text{if } R_1 \geq r. \end{cases} \tag{6}$$

Parameters R_0 and R_1 are given such that $0 < R_0 < R_1$.

We seek an approximate displacement field of the following form:

$$u_h = \sum_{1 \leq i \leq N} a_i\, \varphi_i + \sum_{i \in I_H} b_i\, H\varphi_i + \sum_{1 \leq j \leq 4} c_j\, F_j \chi. \tag{7}$$

The degrees of freedom are vector-valued: $a_i, b_i, c_j \in \boldsymbol{R}^2$. The corresponding discrete problem is the following: find u_h such that

$$u_h \in V_h,\ \ a(u_h, v_h) = L(v_h) \quad \forall v_h \in V_h, \tag{8}$$

where V_h is the vector space of the displacements of the form (7).

The present method differs from the standard *XFEM* by the definition of the singular enrichment term. Namely, for the classical extended finite element, the last term in expression (7) of the approximate displacement u_h is changed into:

$$\sum_{i\in I_F}\sum_{1\le j\le 4} c_{ij}\ F_j\psi_i, \quad c_{ij}\in \boldsymbol{R}^2, \tag{9}$$

where the local *partition of unity* ψ_i $(i \in I_F)$ is equal to the *linear* finite element basis functions associated to the vertices of the element containing the crack tip x^*. A variant consists in enriching all the finite elements nodes in a fixed area around x^*, say the disk $B(x^*, R)$ of radius $R > 0$ independent of h. The crack tip enrichment term then becomes:

$$\sum_{i\in I_F(R)}\sum_{1\le j\le 4} c_{ij}\ F_j\psi_i, \tag{10}$$

where $I_F(R)$ corresponds now to the nodes in $B(x^*, R)$ [3, 11].

In the following result of convergence, the exact solution u satisfies the smoothness condition:

$$u - u^* \in \boldsymbol{H}^{2+\epsilon}(\Omega), \tag{11}$$

for some $\epsilon > 0$ (see (3)). In the statement below, only the case $k = 1$ is considered. To our knowledge, this is the first mathematical result about the accuracy of *XFEM* type methods [4, 5].

Theorem 1. *Let u be the displacement field solution to the model problem (1) on the cracked domain, and u_h the discrete solution defined from the enriched linear finite element method (7), (8). Under assumption (11), the following error estimate holds:*

$$\|u - u^h\|_{1,\Omega} \le Ch\|u - \chi u^*\|_{2+\epsilon,\Omega}, \tag{12}$$

where u^* is the asymptotic displacement (2) at the crack tip x^*, χ the cut-off function for the singular enrichment and $C > 0$ a constant only depending on Ω.

Remark 1. For a classical affine finite element method over a cracked domain, the error is of order $\sqrt{h}$, since the displacement field belongs to $H^{3/2-\epsilon}$ for any $\epsilon \ge 0$. The error estimate obtained in Theorem 1 is *optimal* in the sense that the rate of convergence is the same than using a classical P_1 finite element method for a *smooth* problem (the presence of $\epsilon > 0$ in the assumption (11) only corresponds to a technical difficulty).

The numerical tests are relative to the model problem (1) on the square domain $\overline{\Omega} = [-0.5, 0.5] \times [-0.5, 0.5]$ where the crack is the line segment $\Gamma_C = [-0.5, 0] \times \{0\}$. The exact solution u is the mode I crack displacement (4) prescribed as a Dirichlet condition on the whole domain boundary. The parameters of the cut-off function χ in the definition (6) are equal to $R_0 = 0.01$, $R_1 = 0.49$ and $\chi(x)$ is identical to a

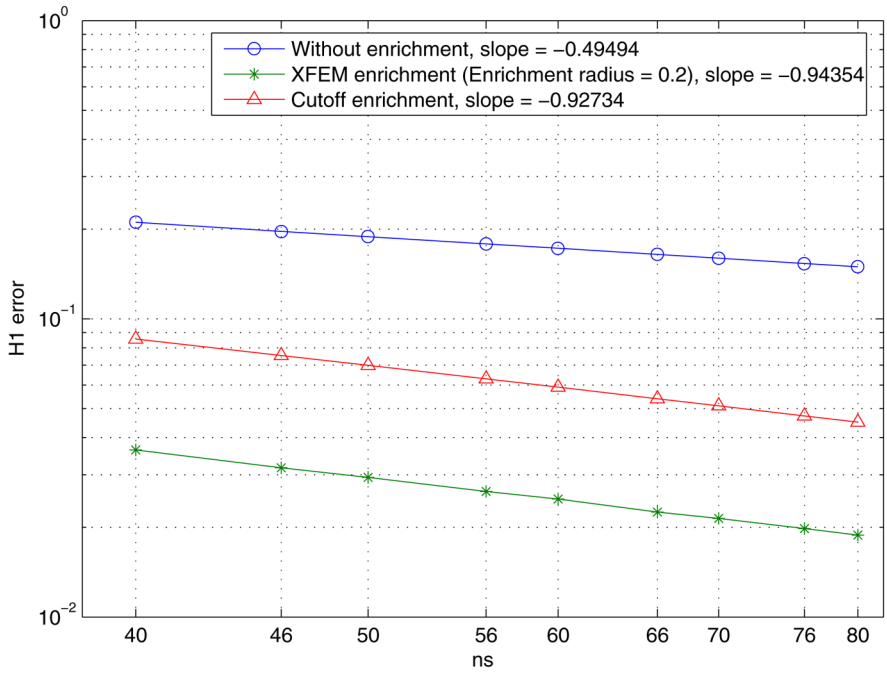

Fig. 2. Energy norm error for classical or enriched P1 elements with respect to the number of cells $ns = 1/h$ in each direction (logarithmic scales).

fifth degree polynomial if $R_0 \leq |x - x^*| \leq R_1$. The triangulation of the domain is defined from a grid of square cells (independently of the crack); let ns be the number of cells of the subdivision in each direction. A linear Lagrange finite element method is considered on $\mathcal{T}_h$.

Figure 2 shows a comparison between the convergence rates of:

- the classical finite element method (without enrichment),
- the *XFEM* method specified by (10), where the radius of the singular enrichement area is equal to $R = 0.2$,
- the previous cut-off enrichment strategy.

The energy norm error $\|u - u_h\|_{1,\Omega}$ is computed by running the test problem for different values of the mesh parameter $h = 1/ns$. It may be seen that the numerical error is of order h^α where the slope α on the figure differs according to the method. With respect to the classical finite element method, the cut-off enrichment reduces the error for a given mesh and presents a convergence rate α almost equal to 1 instead of 1/2. Compared to the *XFEM* method with a fixed enrichment area, the convergence rate is very close, but the computational cost is better in the case

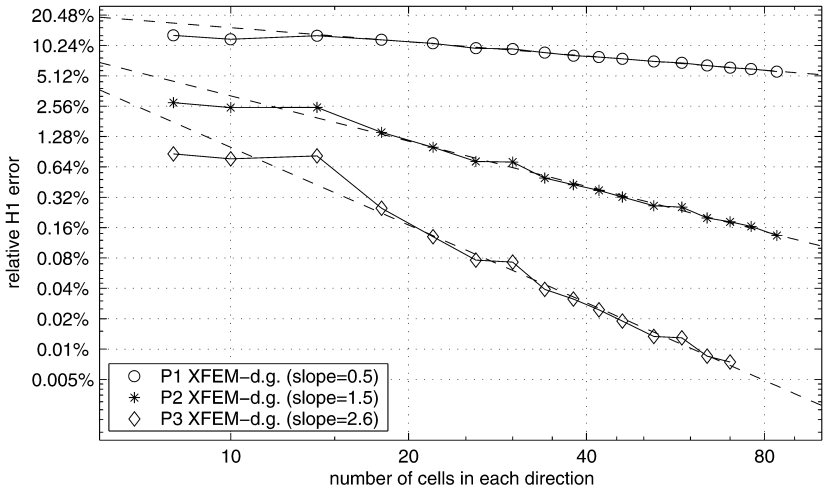

Fig. 3. Energy norm error with respect to $1/h$ in the case of the modified *XFEM* method using a finite element cut-off function (*XFEM*–d.g.).

of the cut-off method. In fact, the number of degrees of freedom increases significantly when h goes to zero in the term (10) specific to *XFEM* with a fixed enrichment area. Another advantage of the cut-off method lies in its significantly better condition number. Further details can be found in [5].

4 Piecewise Linear Cut-Off Function

The cut-off function is now defined as the continuous piecewise linear function on the finite element mesh, which is equal to 1 at the vertices in $B(x^*, R)$ and 0 at the other ones. It is denoted:

$$\chi_h = \sum_{i \in I_F(R)} \psi_i \tag{13}$$

with the previous notations. The approximate displacement considered is now written:

$$u_h = \sum_{1 \le i \le N} a_i \, \varphi_i + \sum_{i \in I_H} b_i \, H\varphi_i + \sum_{1 \le j \le 4} c_j \, F_j \chi_h \tag{14}$$

and the degree k of the finite element basis functions φ_i here is equal to 1, 2 or 3.

For the Mode I test problem considered in the previous section, the convergence curves are given on Figure 3. The radius R of the enrichment area is fixed to $1/10th$ of the domain size. The figure shows that the convergence rate is equal to 0.5, 1.5, 2.6 according to the different choices of the polynomials degree $k = 1, 2, 3$ respectively.

Let us observe that the rate of convergence is equal to 0.5 whatever the degree k in the classical *XFEM* method [11, 18].

Some comments about the method under consideration may be made.

(i) The crack tip term in the approximate displacement u_h for the method of the piecewise linear cut-off function:

$$\sum_{j=1}^{4} c_j \; F_j \, \chi_h \tag{15}$$

has to be compared to the corresponding term for *XFEM* with a fixed enrichment area (10). The cut-off enrichment (15) may be interpreted as a *bonding condition* between the enrichment degrees of freedom of the other method, or a d.o.f. gathering (XFEM–d.g.).

(ii) About the second term in the approximate displacement (14), the partition of unity for H is defined by the P_k finite element basis functions φ_i instead of the P_1 partition of unity ψ_i in the standard *XFEM*. So the approximation of the jump $[u_h]$ of displacement along Γ_C:

$$[u_h] = 2 \sum_{i \in I_H} b_i \, \varphi_i \quad \text{on} \;\; \Gamma_C$$

is compatible with the finite element method (i.e. of the same order).

(iii) In the chosen approximation strategy (14), the number of degrees of freedom for the F_j enrichment is minimal for a given enrichment aera $B(x^*, R)$. Moreover, the condition number is significantly better than using a classical *XFEM* enrichment on a fixed subdomain (when h decreases and for high degree k) [11]. An explanation may be found in the fact that the enrichment functions are not linearly independent. For instance, in the case of a P_1 partition of unity, we observe that

$$p_2(F_1 - F_4) + p_1 F_3 = 0, \quad p_2(F_3 - F_2) + p_1 F_4 = 0,$$

where p_i are the linear shape functions on the reference triangle:

$$p_1(x, y) = x, \;\; p_2(x, y) = y \;\; \text{and} \;\; p_3(x, y) = 1 - x - y.$$

If a P_2 partition of unity is used, there are six relations of that kind.

5 The Polar Numerical Integration

Special care has to be taken in the numerical integration of the elementary stiffness matrix for the triangle containing the crack tip. First, expressing the integral

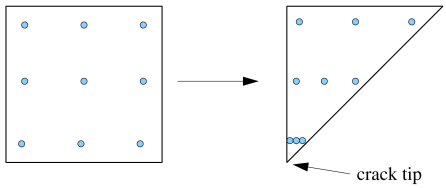

Fig. 4. Transformation of an integration method on a square into an integration method on a triangle for crack-tip functions.

$$\int_T \nabla(F_i\varphi_j).\nabla(F_k\varphi_l)\,dx$$

in polar coordinates, the $r^{-1/2}$ singularity of $\nabla F_i(x)$ is canceled. The finite element is then divided in (a few number of) subtriangles such that the crack tip is a vertex of some of them. For such subtriangles, the following integration method gives excellent results with a low number of integration points (keeping a classical Gaussian curvature formulae on the other subtriangles).

The geometric transformation $\tau : (x_1, x_2) \to (x_1x_2, x_2)$ maps the unit square onto a triangle (Figure 4). Using this transformation, it is possible to build a curvature formulae on the triangle from each one defined on the unit square. The new integration points $\bar{\xi}$ and their weights $\bar{\eta}$ are obtained from those of the original curvature formulae by

$$\bar{\xi} = \tau(\xi), \quad \bar{\eta} = \eta \det(\nabla\tau).$$

This curvature formulae will be called in the following the *polar integration* method.

The performances of the classical refined numerical integration and the polar integration curvature formulae are compared computing a *XFEM* elementary matrix. The reference elementary matrix is computed on a very refined subdivision near the singularity point x^*. Figure 5 presents the relative error in infinity norm between this reference elementary matrix and a computation of the elementary matrix by the following different strategies:

- using a regular refinement of the triangle and a fixed Gaussian formulae on each refined triangle (of order 3 and 10),
- using the polar integration method without any refinement, but for Gaussian curvatures on the square of increasing order.

This figure shows that the polar integration approach offers an important gain. Practically, 25 Gauss points were enough for the most accurate convergence test we have done.

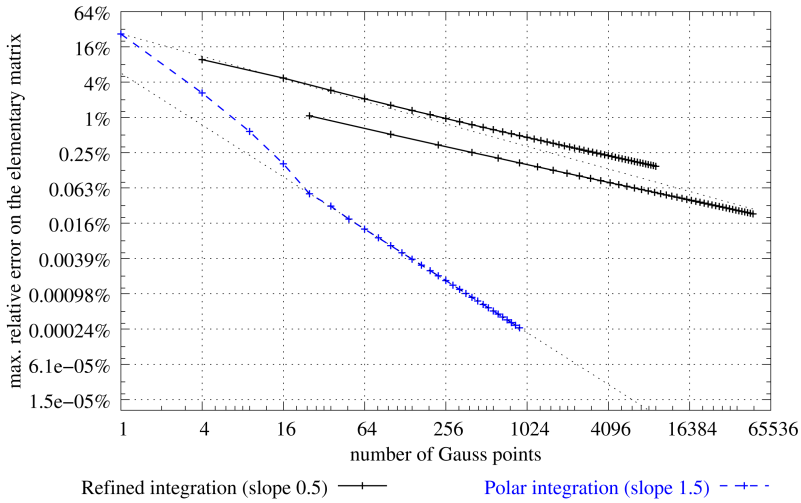

Fig. 5. Comparison of numerical integration methods for nonsmooth functions: uniform refinement with order 3 or 10 Gaussian method, and polar integration.

6 Pointwise Matching at the Boundary of Enriched Zone

The rates of convergence obtained in Figure 3 are not optimal. The only potential problem comes from the *transition layer* between the enrichment area and the rest of the domain, i.e. the triangles partially enriched. An analysis of interpolation error shows a lack of accuracy of *XFEM* methods due to the transition layer [11]. Let us note that a different analysis of this kind of problem is done in [6] where a specific *reproducing condition* is introduced. But this analysis cannot be straightforwardly applied to the present problem.

Let Ω^1 and Ω^2 be a partition of Ω where Ω^i is a union of mesh triangles, the crack tip belonging to Ω^2. The interface between Ω^1 and Ω^2 is denoted Γ_{12}. The approximate displacement u_h is such that $u_h = u_h^1$ on Ω^1 *without* a F_j enrichment:

$$u_h^1 = \sum_{i \in I(\Omega^1)} a_i \, \varphi_i + \sum_{i \in I_H(\Omega^1)} b_i \, H\varphi_i$$

and $u_h = u_h^2$ on Ω^2 *with* a F_j enrichment:

$$u_h^2 = \sum_{i \in I(\Omega^2)} a_i \, \varphi_i + \sum_{i \in I_H(\Omega^2)} b_i \; H\varphi_i + \sum_{j=1}^{4} c_j \, F_j .$$

Finally, $u_h^1 = u_h^2$ at the nodes on Γ_{12}. Naturally, this approximation procedure is no longer a conformal method. The matching condition at the interface may be seen

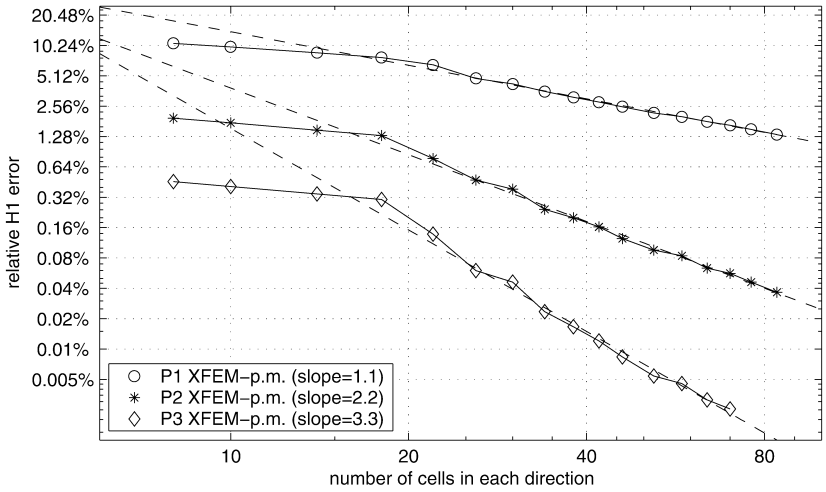

Fig. 6. Convergence of *XFEM* with pointwise matching condition (*XFEM*–p.m.) for the mode I problem.

as a linear relation between the concerned degrees of freedom from the one or the other side of Γ_{12}. The convergence curves in Figure 6 show that optimality is reached (actually, with a slight superconvergence) without any increasing of the number of degrees of freedom or making the condition number worse. For more details, see [11].

Remark 2. The *XFEM* method is based on a partition of unity principle. The *Partition of Unity Finite Element Method* does not exhibit such a lack of accuracy [14] [1] [7]. Thus, an idea is to be closer to *PUFEM* original principle. So let consider a *PUFEM* method using two overlapping subdomains Ω^1 and Ω^2 such that the crack tip x^* belongs to Ω^1 but not to $\bar{\Omega}^2$; a *XFEM* enrichment is defined on Ω^1 with a standard finite element approximation on Ω^2. This method is different from the classical *XFEM* only on the transition layer. It may be seen that the size of the transition layer does not influence the interpolation error estimate and consequently the convergence rate. So a transition layer with a vanishing width should be convenient (i.e. when Ω^1 and Ω^2 define a partition of Ω): this is the motivation of the previous *XFEM* method with pointwise matching.

The numerical experiments were performed with the finite element library *Getfem++* [17].

References

1. I. Babuška and J. M. Melenk. The Partition of Unity Method. *Int. J. Numer. Meth. Engng.*, 40:27–758, 1997.
2. T. Belytschko, N. Moës, S. Usui and C. Parimi. Arbitrary discontinuities in finite elements. *Int. J. Numer. Meth. Eng.*, 50(4): 993–1013, 2000.
3. E. Béchet, H. Minnebo, N. Moës and B. Burgardt. Improved implementation and robustness study of the X-FEM for stress analysis around cracks. *Int. J. Numer. Meth. Engng.*, 64:1033–1056, 2005.
4. E. Chahine, P. Laborde, Y. Renard. A quasi-optimal convergence result for fracture mechanics with XFEM. *C. R. Acad. Sci., Paris*, Ser. I, 342:527–532, 2006.
5. E. Chahine, P. Laborde, Y. Renard. Crack tip enrichment in the XFEM method using a cut-off function. *Submitted.*
6. J. Chessa, H. W. Wang, T. Belytschko. On construction of blending elements for locally partition of unity enriched finite element methods. *Internat. J. Numer. Meth. Engr.*, 57(7):1015–1038, 2003.
7. C.A.M. Duarte, I. Babuška and J.T. Oden. Generalized finite element method for three-dimensional structural mechanics problems. *Computers and Structures*, 77:219–232, 2000.
8. A. Gravouil, N. Moës and T. Belytschko. Non-planar 3D crack growth by the extended finite element and level sets, Part II: Level set update. *Int. J. Numer. Meth. Eng.*, 53(11): 2569–2586, 2002.
9. P. Grisvard. *Singularities in Boundary Value Problems*. Masson, 1992.
10. P. Grisvard. Problèmes aux limites dans les polygones – Mode d'emploi *EDF Bull. Direction Etudes Rech. Série C Math. Inform.*, 1:21–59, 1986.
11. P. Laborde, Y. Renard, J. Pommier and M. Salaün. High order extended finite element method for cracked domains. *Int. J. Numer. Meth. Engng.*, 64:354–381, 2005.
12. J. B. Leblond. *Mécanique de la Rupture Fragile et Ductile*. Hermes, Lavoisier, 2003.
13. J. Lemaitre and J.-L. Chaboche *Mechanics of Solid Materials*. Cambridge University Press, 1994.
14. J.M. Melenk and I. Babuška. The partition of unity finite element method: Basic theory and applications. *Comput. Meth. Appl. Mech. Engng.*, 139:289–314, 1996.
15. N. Moës, J. Dolbow, and T. Belytschko. A finite element method for crack growth without remeshing. *Int. J. Numer. Meth. Engng.*, 46:131–150, 1999.
16. N. Moës, A. Gravouil and T. Belytschko. Non-planar 3D crack growth by the extended finite element and level sets, Part I: Mechanical model. *Int. J. Numer. Meth. Engng.*, 53(11):2549–2568, 2002.
17. J. Pommier and Y. Renard. Getfem++. *An Open Source generic C++ library for finite element methods*, http://www.gmm.insa-toulouse.fr/getfem.
18. F.L. Stazi, E. Budyn, J. Chessa and T. Belytschko. An extended finite element method with higher-order elements for curved cracks. *Comput. Mech.*, 31:38–48, 2003.
19. N. Sukumar, N. Moës, B. Moran and T. Belytschko. Extended finite element method for three dimensional crack modelling. *Int. J. Numer. Meth. Engng.*, 48:1549–1570, 2000.